Unique Binding Site for Mn^{2+} Ion Responsible for Reducing an Oxidized Y_Z Tyrosine in Manganese-Depleted Photosystem II Membranes†

Taka-aki Ono*,‡,§ and Hiroyuki Mino‡

Laboratory for Photo-Biology, RIKEN Photodynamics Research Center, The Institute of Physical and Chemical Research, 19-1399 Koeji, Nagamachi, Aoba, Sendai 980-0868, Japan, and Photosynthesis Research Laboratory, The Institute of Physical and Chemical Research (RIKEN), Wako, Saitama 351-0198, Japan

Received December 15, 1998; Revised Manuscript Received April 19, 1999

ABSTRACT: Binding of Mn^{2+} to manganese-depleted photosystem II and electron donation from the bound Mn^{2+} to an oxidized Y_Z tyrosine were studied under the same equilibrium conditions. Mn^{2+} associated with the depleted membranes in a nonsaturating manner when added alone, but only one Mn^{2+} ion per photosystem II (PS II) was bound to the membranes in the presence of other divalent cations including Ca^{2+} and Mg^{2+}. Mn^{2+}-dependent electron donation to photosystem II studied by monitoring the decay kinetics of chlorophyll fluorescence and the electron paramagnetic resonance (EPR) signal of an oxidized Y_Z tyrosine (Y_Z^+) after a single-turnover flash indicated that the binding of only one Mn^{2+} ion to the manganese-depleted PS II is sufficient for the complete reduction of Y_Z^+ induced by flash excitation. The results indicate that the manganese-depleted membranes have only one unique binding site, which has higher affinity and higher specificity for Mn^{2+} compared with Mg^{2+} and Ca^{2+}, and that Mn^{2+} bound to this unique site can deliver an electron to Y_Z^+ with high efficiency. The dissociation constant for Mn^{2+} of this site largely depended on pH, suggesting that a single amino acid residue with a pK_a value around neutral pH is implicated in the binding of Mn^{2+}. The results are discussed in relation to the photoactivation mechanism that forms the active manganese cluster.

Photosynthetic oxygen is evolved by a catalytic reaction of a tetranuclear manganese cluster located in the lumenal side of photosystem II (PS II)[1] protein complex. However, details of the mechanism of water photooxidation that produces molecular oxygen, the structure of the manganese cluster, and the protein matrixes responsible for coordinating the cluster are still quite limited (reviewed in refs *1*−*4*). One unique feature of the formation of the manganese cluster is that the photochemical process known as photoactivation is involved. Extensive kinetic studies of photoactivation in variously different experimental systems indicate that this process consists of at least two photochemical events with several intermediate reaction states (*5*−*9*). According to the two-quantum hypothesis for photoactivation (*7*), Mn^{2+} bound to a specific binding site is photooxidized, followed by the sequential binding and photooxidation of another Mn^{2+} ion, and two other Mn^{2+} ions are incorporated to complete the tetranuclear cluster. Formation of the active cluster required Ca^{2+} (*10*, *11*), which is also an indispensable inorganic cofactor for oxygen evolution, although the effects of Ca^{2+} ion on the process of the photoactivation are rather contradictory (*8*, *9*, *11*, *12*). Ca^{2+} may be involved in formation of the active cluster according to a photoactivation study that used an ionophore for divalent cations (*11*). Later, it was found that the tetranuclear cluster can be formed in the absence of Ca^{2+}, although oxygen evolution capability requires Ca^{2+} (*8*, *12*). On the other hand, Ca^{2+} has been reported to be required for formation of the tetranuclear cluster at near-stoichiometric concentrations of Mn^{2+} (*9*).

In Mn-depleted PS II obtained by washing with NH_2OH or Tris, an exogenously added Mn^{2+} donates an electron to PS II (*13*−*20*). This reaction was regarded as the first photochemical process constituting photoactivation, and a binding site of Mn^{2+} is considered to overlap or is closely correlated with the native ligation site of the manganese cluster. In fact, several site-directed and spontaneous mutations that were assumed to modify around the putative ligation site for the manganese cluster and Y_Z tyrosine have found to alter the ability to oxidize Mn^{2+} (*21*, *22*). The properties of Mn^{2+} oxidation have been extensively studied with a view to elucidating the mechanism of photoactivation as well as to identifying the ligation site of the manganese cluster. The binding of Mn^{2+} has been estimated by the ability of Mn^{2+} to donate an electron to PS II determined by monitoring DCIP photoreduction with Mn^{2+} (*13*−*16*, *20*, *21*), Mn^{2+}-dependent inhibition of electron donation from DPC (*23*, *24*, *25*), Mn^{2+}-dependent stimulation of electron donation

† This work was supported by grants for Frontier Research Program and Photosynthetic Science at RIKEN given by the Science and Technology Agency of Japan and by a Grant-in-aid for Science Research on Priority Area (10129233) and by a Grant-in-Aid for Scientific Research (09640783) from the Ministry of Education, Science and Culture of Japan. H.M. was supported by grants for special postdoctoral research from RIKEN.

* To whom correspondence should be addressed: Fax +81 22 228 2045; E-mail takaaki@postman.riken.go.jp.

‡ Laboratory for Photo-Biology, RIKEN Photodynamics Research Center.

§ Photosynthesis Research Laboratory, RIKEN.

[1] Abbreviations: Chl, chlorophyll; DCMU, 3-(3,4-dichlorophenyl)-1,1-dimethylurea; DPC, 1,5-diphenylcarbazide; DCIP, 2,6-dichlorophenolindophenol; EPR, electron paramagnetic resonance; Mes, 2-(*N*-morpholino)ethanesulfonic acid; PS II, photosystem II; Y_Z, redox-active tyrosine 161 of the D1 protein; Q_A, primary quinone acceptor of photosystem II.

10.1021/bi982949s CCC: $18.00
Published on Web 06/17/1999

from hydrogen peroxide (*14*−*16*), Mn^{2+}-dependent change in the yield and decay kinetics of Chl a fluorescence (*21*, *26*−*29*), and the Y_Z^+ EPR signal (*17*, *20*). Studies using stoichiometric amounts of Mn^{2+} indicate that adding two or more Mn^{2+} ions per PS II facilitates electron donation from Mn^{2+}, suggesting that at least two Mn^{2+} ions must bind per PS II for effective electron transfer (*16*, *27*, *30*). Mn^{2+} binding to multiple sites with different levels of affinity and various chemical properties has been suggested through kinetic analysis of electron donation by Mn^{2+} combined with changes of the putative sites using chemical modifiers specific for amino acid residues (*20*, *23*, *28*, *29*, *31*) and by selective proteolysis (*24*). Furthermore, an EPR signal attributable to a binuclear Mn(II,II) cluster was detected as a precursor of the active tetranuclear cluster formed by photoactivation when both Mn^{2+} and Ca^{2+} were added to Mn-depleted PS II in the dark (*30*). These results imply that original or portions of the original ligation sites for the native cluster exist even in Mn-depleted PS II.

Although these analyses may provide some information about the Mn^{2+} binding responsible for electron donation, the amounts of Mn^{2+} bound to PS II under equilibrium conditions should be directly quantified to characterize the binding of Mn^{2+} and the electron donation from the bound Mn^{2+}. However, very few attempts have been made to elucidate the amounts of Mn^{2+} associated with Mn-depleted PS II (*16*, *24*). In this study, the amount of Mn^{2+} bound to the Mn-depleted PS II was directly determined, and the electron donation from Mn^{2+} was examined by monitoring Chl a fluorescence and the Y_Z^+ EPR signal under the conditions of the Mn^{2+} binding assay. The Mn^{2+} oxidation were measured by a single-flash condition, which prevents possible interference by Mn^{3+} generated during photochemical measurements. The results show that Mn-depleted PS II retains only one high-affinity/high-specificity site for Mn^{2+} and that Mn^{2+} bound to this site is selectively photooxidized by Y_Z^+. Some properties of this unique binding site are also presented.

MATERIALS AND METHODS

Biochemical Preparations. Oxygen-evolving PS II membranes were prepared from spinach as described (*32*). The membranes were depleted of Mn by washing with NaCl/NH_2OH or Tris/NH_2OH. To wash with NaCl/NH_2OH, the membranes were suspended in medium consisting of 2 M NaCl, 0.4 M sucrose, and 20 mM Mes/NaOH (pH 6.5) at 1 mg of Chl/mL and incubated for 20 min at 0 °C. The membranes were then suspended in medium consisting of 0.4 M sucrose, 20 mM NaCl, 1 mM NH_2OH, and 20 mM Mes/NaOH (pH 6.5) at 1 mg of Chl/mL after one wash each with the 2 M NaCl buffer and the 20 mM NaCl buffered media. After an incubation for 5 min at 0 °C, 1 mM NaEDTA was added to the sample suspension. The membranes were extensively washed with the same medium without NaEDTA to eliminate NaEDTA completely. After 5 washes, the membranes were suspended in a medium containing 0.4 M sucrose, 20 mM NaCl, and 20 mM Mes/NaOH (pH 6.5) (buffer A) and stored in liquid N_2. To wash with Tris/NH_2OH, the membranes were incubated in 30 mM Tris-HCl (pH 9.7) at 0.5 mg of Chl/mL for 10 min at 0 °C. The membranes were immersed in the medium containing 1 mM NH_2OH followed by extensive washes as described above and then resuspended in buffer A. Nontreated control membranes were washed once with buffer A containing 1 mM NaEDTA and then resuspended in buffer A after extensive wash. Oxygen-evolving activity was not changed by this procedure in control membranes.

Mn Quantification. For binding studies, NaCl/NH_2OH-treated and Tris/NH_2OH-treated membranes were suspended in buffer A containing various concentrations of $MnCl_2$ at 1 mg of Chl/mL. $CaCl_2$ or $MgCl_2$ was added where indicated. After an incubation for 10 min at 20 °C, the membranes were removed from the suspension by centrifugal filtration through 0.65 μm filter units (Ultrafree, Millipore). The amount of Mn^{2+} in the filtrate was determined by measuring the intensity of the six-line EPR signal of Mn^{2+} with a Jeol JES-FE1XG X-band EPR spectrometer using a flat-type cell (70 μL) at 20 °C. The microwave power was 10 mW, and the modulation frequency and amplitude were 100 kHz and 20 G, respectively. The amount of bound Mn^{2+} was estimated by subtracting free Mn^{2+} from the total. To determine the Mn content of the control, the NaCl/NH_2OH-treated, and Tris/NH_2OH-treated membranes, Mn was extracted with 0.2 M HNO_3 and 0.1 M $CaCl_2$ for 20 min at room temperature, followed by centrifugation to precipitate the denatured membranes. Then, the amount of Mn in the supernatant was determined by EPR spectroscopy. Alternatively, the Mn content of the sample membranes was directly determined by atomic absorption as described (*33*). The same results were obtained by these two procedures.

Photoactivation. NaCl/NH_2OH-treated PS II membranes were suspended at 1 mg of Chl/mL in buffer A supplemented with DCIP, $MnCl_2$, $CaCl_2$, and NaCl as indicated. Aliquots of 0.2 mL of sample suspension were distributed to a 7 mm diameter plastic tray and were illuminated with fluorescent white light at 20 °C for 30 min. O_2 evolution was measured with a Clark-type oxygen electrode in buffer A supplemented with 50 mM $CaCl_2$ and 0.5 mM phenyl-*p*-benzoquinone at 25 °C under saturating light conditions.

Fluorescence Decay Kinetics. Fluorescence decay after a single flash was measured with a PAM fluorometer (Waltz, Germany) at 20 °C. Membrane suspensions were excited with a single-turnover flash (8 μs), and the decay kinetics were monitored at 20 and 100 μs resolution with a measuring light at 100 kHz modulation. Sample membranes were placed in a cell with a thickness of 0.1 and 4 mm for measurements at 1 and 0.025 mg of Chl/mL, respectively. DCMU (50 and 20 μM) was added to the sample suspensions at 1 and 0.025 mg of Chl/mL to interrupt Q_A^- oxidation by Q_B.

Y_Z^+ Signal Decay Kinetics. Rereduction kinetics of Y_Z^+ after a single flash were monitored by EPR signal II_f using a Jeol JES-FE1XG X-band EPR spectrometer and a flat-type cell at room temperature. Samples at 1 mg of Chl/mL in buffer A were intermittently conducted into the cell by a peristaltic pump from a reservoir on ice and were illuminated with a 7 ns single pulse from a frequency-doubled (532 nm) Nd−YAG laser (Spectra-Physics) with an energy of about 20 mJ. DCMU (50 μM) was added to the sample suspensions. The laser was fired at 0.2 s after cessation of pumping, EPR data were acquired during the next 1.2 s, and then new samples were supplied by a 0.6 s operation of the pump. The sequence was controlled with a personal computer. The kinetic traces of Y_Z^+ were directly recorded with a digital oscilloscope (LeCroy 9400A) with no capacitive coupling,

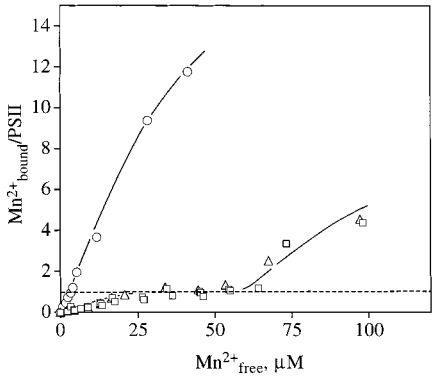

FIGURE 1: Amounts of Mn^{2+} bound to NaCl/NH_2OH−PS II membranes. Medium contained 5 mM $CaCl_2$ (□), $MgCl_2$ (△), and no divalent cation (○) in addition to exogenous $MnCl_2$ at various concentrations. Dashed line corresponds to one Mn^{2+}/PS II. Data are the average of three measurements. Sample membranes at 1 mg of Chl/mL in buffer A (pH 6.5) were incubated with various concentrations of Mn^{2+} and a supplemented divalent cation in the dark. The amounts of free and bound Mn^{2+} were elucidated by determining free Mn^{2+} in filtrates that passed through 0.65 μm membrane filters.

and 1000−1400 traces were averaged. The magnetic field was fixed on the low-field peak of the Y_Z^+ spectrum. Other EPR settings were as follows: time constant, 1 ms; microwave frequency, 9.445 GHz; microwave power, 3 mW; and field modulation amplitude, 20 G at 100 kHz. Identical kinetic data were obtained at a field modulation of 5 G.

RESULTS

Mn^{2+} Binding. NaCl/NH_2OH-treated and Tris/NH_2OH-treated PS II membranes lost almost all manganese (<0.1 Mn/220 Chl) compared with control membranes (4.1 ± 0.2 Mn/220 Chl). The addition of Mn^{2+} ions to the NaCl/NH_2OH-treated membranes caused equilibrium binding of the ion to the membranes as shown in Figure 1. The amounts of bound Mn^{2+} increased with free Mn^{2+} (Mn^{2+}_{free}) in a non-saturating manner, indicating that the membranes possess multiple sites for Mn^{2+} with heterogeneous binding properties. These findings are consistent with the fact that the intensity of the aqueous six-line EPR spectrum becomes negligibly small when stoichiometric amounts of Mn^{2+} are added to the membranes (*34*). It is of note in this context that we could not detect a Mn^{2+}-binding site with submicromolar affinity in this assay. Our results are contrast to the finding (*16*, *24*) that limited numbers of Mn^{2+} (1−3 Mn^{2+}/PS II) are bound to Mn-depleted PS II. Although the reason for this contradiction is unknown at present, it may be significant that the metal assays had been conducted after illumination of the samples with continuous light in the presence of Mn^{2+}. Chen et al. (*35*) have reported that Mn^{2+} is incorporated into Mn-depleted membranes after illumination in the presence of Mn^{2+} but without Ca^{2+}, although O_2 evolution activity is not restored. Therefore, the reported amount of bound Mn may reflect Mn^{2+} incorporated into the membranes in a light-dependent manner. The binding curve was markedly changed in the presence of 5 mM Ca^{2+}, which may be associated with the putative Mn^{2+}-binding sites as a specific competitor and/or reduce the local concentration of Mn^{2+} effected by surface charges around the putative binding sites. Binding of Mn^{2+} was largely suppressed, reaching a plateau around 0.9−1.0 Mn^{2+}/PS II and then increasing gradually above 50 μM Mn^{2+}_{free}. A similar binding curve was obtained in the presence of 5 mM Mg^{2+}, indicating that the effect is not specific for Ca^{2+}. These results indicate that NaCl/NH_2OH-treated PS II membranes have a unique high-affinity binding site with high specificity for Mn^{2+} but most Mn^{2+} weakly and/or nonspecifically binds to the membranes via electrostatic interactions.

Table 1: Restoration of Photosynthetic Oxygen Evolution by Photoactivation in Extensively Washed NaCl/NH_2OH-Treated PS II Membranes

	oxygen-evolving activity	
sample membranes	μmol of O_2 (mg of Chl·h)$^{-1}$	rel %
nontreated control	590	100
NaCl/NH_2OH treated	<10	<2
NaCl/NH_2OH treated and photoactivated[a]		
condition A	430	73
condition B	320	54

[a] NaCl/NH_2OH washed membranes (1 mg of Chl/mL) were illuminated for 30 min in buffer A containing 1 mM $MnCl_2$, 20 mM $CaCl_2$, and 100 mM NaCl for condition A or 50 μM $MnCl_2$, 5 mM $CaCl_2$, and 20 mM NaCl for condition B. DCIP (10 μM) was included in either condition.

Photoactivation. NaCl/NH_2OH-treated PS II membranes used for Mn^{2+}-binding studies showed nearly no O_2 evolution, which is consistent with an almost complete loss of manganese, but O_2 evolution was restored by illuminating the treated membranes as shown in Table 1. Considerable O_2 evolution was restored under the same ion condition as that for the Mn^{2+} binding assay: 50 μM $MnCl_2$, 5 mM $CaCl_2$, and 20 mM NaCl. The Chl concentration used for photoactivation study was identical to that for the Mn^{2+} binding assay. These conditions gave about 45 μM free Mn^{2+}, at which only one Mn^{2+} ion per PS II associated with the membranes before illumination as shown in Figure 1. The restored O_2 evolution under the binding assay condition was as high as 70% of that under the optimum ion condition for photoactivation: 1 mM $MnCl_2$, 20 mM $CaCl_2$, and 100 mM NaCl (*35*−*37*).

Effects of Mn^{2+} on Chl Fluorescence Decay. An electron donation from the bound Mn^{2+} to an oxidized Y_Z (Y_Z^+) was monitored by measuring the yield of flash-induced variable fluorescence in the presence of DCMU as shown in Figure 2. The Chl concentration used for the measurements was identical to that for the Mn^{2+} binding assay shown in Figure 1. A single saturating flash yielded maximum fluorescence level (F_m) due to Q_A^- formation, and the fluorescence yield decayed to a low constant level (F_{Lo}) in the absence of added Mn^{2+} due to the loss of the Q_A^- population by charge recombination between Y_Z^+ and Q_A^-. F_{Lo} was higher than an initial fluorescence level (F_0), presumably due to the presence of an alternative pathway for the reduction of Y_Z^+ and/or P_{680}^+ or the oxidation of a reduced pheophytine. In the presence of Mn^{2+}, the fluorescence decayed to a low stable level (F_L) that reflects the population of the Q_A^- retaining PS II center in which Y_Z^+ is reduced by rapid electron delivery from Mn^{2+}. F_L increased with Mn^{2+} concentration to reach F_m at Mn^{2+} concentrations higher than 8 μM, where the decay was almost completely inhibited due to full reduction of Y_Z^+ by Mn^{2+}. Generally, the relationship between normalized Q_A^- population and fluorescence yield is curvilinear because of energy transfer between PS II units

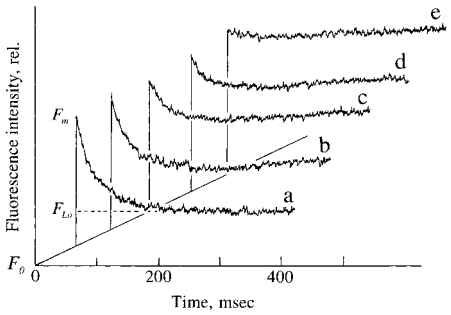

FIGURE 2: Effects of Mn^{2+} on relaxation of the yield of chlorophyll fluorescence. NaCl/NH_2OH-treated PS II membranes at 1 mg of Chl/mL in buffer A (pH 6.5) were illuminated with a single-turnover flash in the presence of (a) 0 μM, (b) 1.4 μM, (c) 3.3 μM, (d) 5.5 μM, and (e) 8 μM Mn^{2+}. DCMU (40 μM) and no divalent cation, other than Mn^{2+} ion, were included in the reaction mixture. Two measurements were averaged. See text for other experimental conditions.

(*38*). This nonlinearity can be minimized, as in the present study, by omitting divalent cation from the reaction mixture (*39*).

Figure 3A shows the effect of the amount of bound Mn^{2+} on the fluorescence that is decayed after a single flash. The relative extent of fluorescence decay, expressed as $(F_m - F_L)/(F_m - F_{Lo})$, decreased in proportion to the number of bound Mn^{2+} ions per PS II and was totally suppressed at 1 Mn^{2+}/PS II. The result indicates that the Y_Z^+ produced by a single flash is rereduced almost completely when one Mn^{2+} is bound to PS II. Since PS II has one unique binding site with high specificity for Mn^{2+} as shown in Figure 1, it is conceivable that the Mn^{2+} bound to this site is preferentially oxidized by Y_Z^+. The result also indicates that Mn^{2+} is oxidized only after binding to this specific site and that $(F_L - F_{Lo})/(F_m - F_{Lo})$ $(= 1 - \{(F_m - F_L)/(F_m - F_{Lo})\})$ reflects the relative population of PS II preserving Mn^{2+}, [Mn^{2+}·PS II]/[PS II_{total}]. Thus, flash-induced photooxidation of Mn^{2+} can be described by the following simple model:

$$[Mn^{2+}_{free}] + [\text{PS II}_{free}] \leftrightarrow [Mn^{2+}\cdot\text{PS II}] \xrightarrow{h\nu} [Mn^{3+}\cdot\text{PS II}]$$

where [Mn^{2+}·PS II] = [Mn^{3+}·PS II].

Figure 3B shows the effect of [Mn^{2+}_{free}] on $(F_m - F_L)/(F_m - F_{Lo})$ measured at 1 mg of Chl/mL (○) and 25 μg of Chl/mL (□). [Mn^{2+}_{free}] can be nearly equal to [Mn^{2+}_{add}] at 25 μg of Chl/mL and be constant before and after a flash, because it can be assumed that [Mn^{2+}·PS II] is negligibly lower than [Mn^{2+}_{add}]. The resulting dependence curves were superimposable despite a 40-fold difference in PS II concentration, indicating that the model and the concomitant assumptions are applicable to the study of Mn^{2+} binding. This also verified the amounts of Mn^{2+} determined in the present study. As shown in the inset figure, the 1/[Mn^{2+}_{free}] vs $1/\{(F_L - F_{Lo})/(F_m - F_{Lo})\}(= 1/\{[Mn^{2+}\cdot\text{PS II}]/[\text{PS II}_{total}]\})$ plot becomes a straight line, the slope of which gives a dissociation constant (K_d) of 1.3 μM that is roughly consistent with the value obtained by a similar method (*28*).

Figure 4 shows the effect of [Mn^{2+}_{free}] on the florescence decay after a single saturating flash in Tris/NH_2OH-treated and NaCl/NH_2OH-treated PS II membranes. The Tris/NH_2OH-treated membranes lost the extrinsic 16, 24, and 33 kDa proteins, whereas the NaCl/NH_2OH-treated membranes preserved the manganese-cluster-stabilizing 33 kDa extrinsic

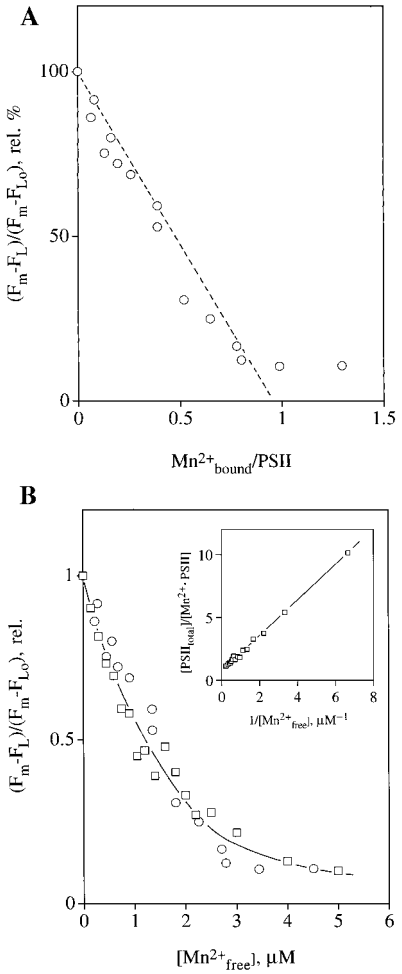

FIGURE 3: (A) Correlation between the relative extent of fluorescence decay after a single flash and the amounts of bound Mn^{2+}. (B) Effects of free Mn^{2+} on the relative extent of fluorescence decay after a single flash. NaCl/NH_2OH-treated PS II membranes at 1 mg of Chl/mL (○) and 25 μg of Chl/mL (□) in buffer A (pH 6.5) were illuminated with a single-turnover flash in the presence of 10 and 40 μM DCMU, respectively. No divalent cation, other than Mn^{2+}, was included in the reaction mixture. The extent of fluorescence decay was expressed as $(F_m - F_L)/(F_m - F_{Lo})$, where F_L, F_{Lo}, and F_m represent a steady-state low fluorescence level after decay in the presence of various concentrations of Mn^{2+}, a steady-state low fluorescence level after decay in the absence of Mn^{2+}, and the maximal fluorescence level, respectively. Inset shows a Scatchard-type plot. See text for other details.

protein but lost the other two proteins. Both of the membrane samples showed the same concentration dependence on [Mn^{2+}_{free}]. Furthermore, Mn^{2+} was bound to the Tris/NH_2OH-treated membranes in the same manner as to the NaCl/NH_2OH-treated membranes (data not shown). These findings indicate that the 33 kDa protein does not influence the affinity of Mn^{2+} for the unique binding site. Thus, the site may be located in a vicinity whose environment is not affected by the 33 kDa protein.

Figure 5 shows the effect of pH on Mn^{2+}-dependent inhibition of fluorescence decay after a single flash. A higher concentration of Mn^{2+} was required for suppression of the fluorescence decay at lower pH values as shown in Figure 5A. Plots of 1/[Mn^{2+}_{free}] vs $1/\{(F_L - F_{Lo})/(F_m - F_{Lo})\}(= 1/\{[Mn^{2+}\cdot\text{PS II}]/[\text{PS II}_{total}]\})$ at respective pH values yielded a straight line despite the obvious change in the concentration dependence curve (Figure 5A, inset). The dissociation

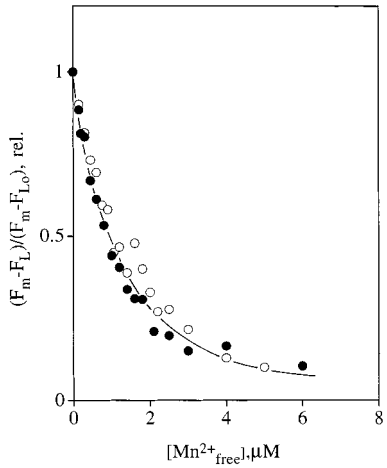

FIGURE 4: Effects of 33 kDa Mn-stabilizing protein on Mn^{2+}-dependent change of the relative extent of fluorescence decay after a single flash. NaCl/NH_2OH-treated (○) and Tris/NH_2OH-treated (●) PS II membranes in buffer A (pH 6.5) were illuminated by a single-turnover flash at 25 μg of Chl/mL in the presence of 10 μM DCMU. No divalent cation, other than Mn^{2+}, was included in the reaction mixture.

constant (K_d) determined by the slope of each line was highly dependent upon pH. The K_d decreased with increasing pH, indicating that the affinity for Mn^{2+} increased with pH. The log K_d vs pH plot shown in Figure 5B reveals that the dependence curve fits a straight line with a slope of approximately −1 below pH 7, and that it is pH-independent above pH 7. The rate of back reaction between Q_A^- and Y_Z^+ after a flash is dependent upon pH with the recombination rate being higher with decreasing pH (*40*, *41*). Therefore, the pH dependence of K_d may reflect the pH-dependent change in the lifetime of Y_Z^+; that is, the probability of the access of Mn^{2+} to Y_Z^+ increased at higher pH values due to the longer lifetime of Y_Z^+. As shown in Figure 5B, pH dependence of the rate of the charge recombination (as the reciprocal of the half-time of fluorescence decay after a flash in the absence of added Mn^{2+}) was considerably different from that of the K_d, being a straight line throughout all pH values with a gentle slope. Therefore, it can be concluded that the observed pH dependence of K_d is attributable to the pH-dependent change in the affinity of the Mn^{2+} binding site. The pH dependence curve suggests that a residue responsible for Mn^{2+} binding has been protonated below pH 7, leading to lower affinity for Mn^{2+}.

Effects of Mn^{2+} on Y_Z^+ Decay. Y_Z^+ reduction by Mn^{2+} was directly measured by following a Y_Z^+ EPR signal after a single flash under the same conditions as those for the Mn^{2+} binding assay and the fluorescence decay experiments. No redox reagent was included in the reaction mixture for elimination of undesirable interaction with Mn^{2+} and/or Mn^{3+}, and the sample was renewed after each flash. Figure 6 shows the effects of Mn^{2+} upon the decay course of the Y_Z^+ signal. Mn^{2+} significantly suppressed the signal intensity as well as the lifetime of Y_Z^+. It is of note that the slow-decaying component found in the absence of Mn^{2+} (trace a) was eradicated by the addition of 7.5 μM Mn^{2+} (trace c).

Figure 7A shows the effects of Mn^{2+} binding on the amplitude of Y_Z^+ signal. The Y_Z^+ amplitude decreased proportionally with increasing amounts of bound Mn^{2+} and lowered to approximately 30% that in the absence of Mn^{2+} at 1 bound Mn^{2+}/PS II. A simple interpretation is that an

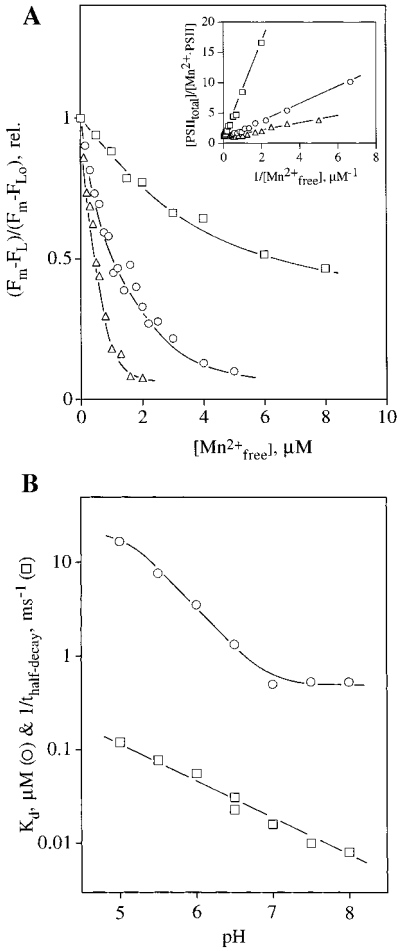

FIGURE 5: (A) Effects of pH on the Mn^{2+} dependence of the relative extent of fluorescence decayed after a single flash. Sample membranes at 25 μg of Chl/mL were incubated in buffered medium at pH 5.5 (□), pH 6.5 (○), and pH 8.0 (△). Inset shows Scatchard-type plots. (B) pH dependence of the Mn^{2+} dissociation constant (○) and the relative rate of charge recombination between Q_A^- and Y_Z^+ in the absence of exogenous Mn^{2+} (□). NH_2OH/NaCl-treated PS II membranes were incubated in buffer medium consisting of 20 mM Mes/NaOH for pH 5.0−6.5 and 20 mM Hepes/NaOH for pH 6.5−8.0. DCMU (10 μM) and no divalent cation, other than Mn^{2+}, were included in the reaction mixture. Dissociation constants were evaluated by the slope of Scachard-type plots shown in the inset of panel A.

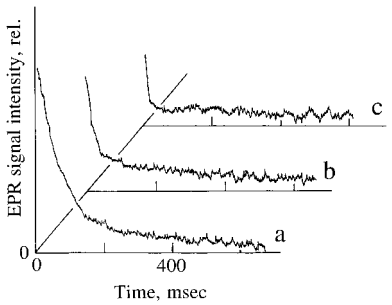

FIGURE 6: Effects of Mn^{2+} on decay kinetics of Y_Z^+ EPR signal after a single-turnover flash in NH_2OH/NaCl-treated PS II membranes. Sample membranes at 1 mg of Chl/mL in buffer A (pH 6.5) were illuminated in the presence of (a) 0, (b) 3, and (c) 7.5 μM Mn^{2+}, respectively. DCMU (50 μM) and no divalent cation, other than Mn^{2+}, were included in the reaction mixture. See text for other details.

electron donation from the Mn^{2+} bound to the unique site is rapid enough to be accomplished within the time constant

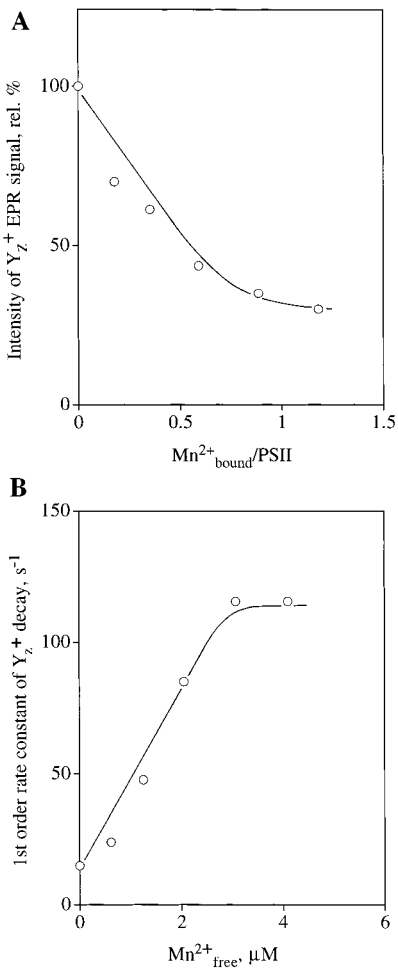

FIGURE 7: (A) Correlation between the intensity of Y_Z^+ EPR signal and the amounts of bound Mn^{2+}. (B) Effects of free Mn^{2+} on the pseudo-first-order rate constant of the decay of Y_Z^+ EPR signal. NH_2OH-treated PS II membranes at 1 mg of Chl/mL in buffer A (pH 6.5) were illuminated with a single-turnover flash in the presence of 50 μM DCMU. No divalent cation, other than Mn^{2+}, was included in a reaction mixture. See text for other details.

of the spectrometer (1 ms), although the broadening of the EPR spectra by binding of Mn^{2+} near Y_Z^+ cannot be excluded completely. The remaining 30% Y_Z^+ can be also ascribed to the PS II center with electron donation from Mn^{2+} because this Y_Z^+ fraction decayed 10 times faster than Y_Z^+ in the absence of Mn^{2+}. The result, therefore, can be interpreted to mean that 30% Y_Z^+ was reduced relatively slowly by Mn^{2+}. Two rationales may explain this. The first is that the rate of electron donation from bound Mn^{2+} to Y_Z^+ is slower in the 30% PS II center, presumably due to modification of the binding site. The second is that Y_Z^+ is reduced by Mn^{2+} in a rather nonspecific manner in the 30% PS II center. These two possibilities may be distinguishable since the rate constant of Y_Z^+ reduction by adventitious Mn^{2+} is expected to increase linearly with Mn^{2+} concentration.

Figure 7B shows the effects of the free Mn^{2+} concentration on the decay rate of the Y_Z^+ signal remaining after rapid reduction by the bound Mn^{2+}. Consistent with the reported results (*17, 20*), Y_Z^+ was reduced with pseudo-first-order kinetics. A pseudo-first-order rate constant showed a linear relationship with free Mn^{2+} at lower concentrations, but the dependence curve bent to a constant level at Mn^{2+} concentrations higher than about 3 mM. The results indicate that the reduction no longer follows a second-order process and is not determined by diffusion and/or collision processes between Y_Z^+ and free Mn^{2+} at these concentrations. It is notable that approximately one Mn^{2+} binds to PS II at 3 μM free Mn^{2+} under experimental conditions. The results, therefore, seems to support the view that Y_Z^+ is directly reduced by Mn^{2+} bound to the specific site even in the 30% PS II center, although the rate of Y_Z^+ reduction is relatively slow.

DISCUSSION

The present results demonstrated that the Mn-depleted PS II membranes have only one binding site with high specificity for Mn^{2+} as shown in Figure 1, although large amounts of Mn^{2+} may associate with the membranes via electrostatic interactions. Since Y_Z^+ is efficiently extinguished by reduction when one Mn^{2+} ion is bound to one unit of PS II as shown by the analyses of flash-induced fluorescence (Figure 3) and the Y_Z^+ EPR signal (Figure 7), the binding site for Mn^{2+} responsible for Y_Z^+ reduction retains higher affinity for Mn^{2+} ions than other nonspecific sites. These findings indicate that Mn-depleted PS II membranes have a unique binding site for Mn^{2+} and that only Mn^{2+} bound to this site is efficiently oxidized by Y_Z^+. It is highly likely that this site corresponds to the high-affinity Mn-binding site suggested by kinetic analyses of Mn^{2+} oxidation (*15, 18, 20, 22, 23, 28*).

Since oxygen-evolving PS II retains the tetranuclear manganese cluster, a maximum of four Mn^{2+} binding sites related to the ligation of the native manganese cluster will exist in the Mn-depleted PS II. Although no direct evidence shows that the Mn^{2+} oxidizing site found in the manganese-depleted PS II comprises the proper site for ligating the manganese cluster, the site is believed to be involved in the first photochemical step in photoligation of the active cluster (*5*−*9*). Therefore, the Mn^{2+} oxidizing site must at least be in very close proximity to the native ligation sites of the manganese cluster. According to one model of photoligation of the active manganese cluster (*7*), a Mn^{2+} ion is oxidized at its binding site by the first photochemical step, then another Mn^{2+} ion is oxidized by a second photochemical step, followed by the binding of two more Mn^{2+} ions. The NaCl/NH_2OH-treated membranes retained high ability to photoligate the active manganese cluster, and 70% O_2 evolution was restored by illumination in the presence of 50 μM Mn^{2+} and 5 mM Ca^{2+} at 1 mg of Chl/mL compared with that restored under optimum ion conditions as shown in Table 1. Since the membranes retained only 1 Mn^{2+} ion/PS II under these conditions in the dark as shown in Figure 1, the present results provide direct evidence that only one Mn^{2+} stably binds to the unique oxidizing site and that the other three Mn^{2+} ions cannot associate with their putative binding sites, at least during the first photochemical step of photoligation of the manganese cluster in accordance with the proposed scenario (*7*). Since four Mn^{2+} ions have to be taken up for the photoactivation, a new high-affinity binding site(s) for Mn^{2+} or Mn^{3+} should be formed as a consequence of the Mn^{2+} oxidation. Alternatively, Mn^{3+} will be oxidized to Mn^{4+} at the same binding site by the second photochemical reaction.

Some reports indicate that Mn^{2+} efficiently donates an electron only when Mn^{2+} is present at a concentration

equivalent to 2 Mn^{2+}/PS II in the presence of $MgCl_2$ and $CaCl_2$ as detected by the recovery of variable fluorescence under continuous light (*26*) and suppression of Y_Z^+ signal formation under multiple flashes (*30*). These results had been interpreted to mean that the binding of 2 Mn^{2+}/PS II facilitates an electron donation to Y_Z^+ from the bound Mn^{2+}. In addition, an EPR signal probably responsible for a spin-coupled binuclear Mn(II,II) has been observed in the dark in the presence of Mn^{2+} added at a concentration equivalent to 2 Mn^{2+}/PS II to the membranes depleted of Mn by a lipophilic chelator (*30*). Since the signal was detectable only in the presence of Ca^{2+}, it has been proposed that Ca^{2+} organizes the Mn(II,II) dimer by interacting directly via solvent or protein-derived bridging ligands and that the Ca^{2+}-induced Mn(II,II) dimer serves as a precursor for the formation of the functional manganese cluster during photoactivation. However, the amount of Mn^{2+} bound to the membranes had never been determined. In fact, only one Mn^{2+} was bound to the membranes in the presence of Ca^{2+} as shown in Figure 1. The proposed dimer, therefore, was not apparently formed in the NaCl/NH_2OH-treated membranes even in the presence of Ca^{2+}. This suggests that the dimer is not a direct precursor for the active manganese cluster during photoactivation. The possibility that the dimer is formed in a minor population of PS II centers under our experimental conditions cannot be completely excluded.

The effects of exogenous Mn^{2+} on Y_Z^+ reduction in Mn-depleted PS II have been previously reported, where the reduction rate of Y_Z^+ is increased by Mn^{2+} addition but the signal amplitude is kept constant (*17, 20*). These results indicate that the rate-determining step of Y_Z^+ reduction is the diffusion of Mn^{2+} to Y_Z^+. On the other hand, Mn^{2+} notably suppressed the intensity of the Y_Z^+ signal and accelerated its decay rate as shown in Figure 6. Since the minimal half-decay time of Y_Z^+ in the presence of Mn^{2+} is reported to be about 2.5 ms (*17*) and 5 ms (*20*), the limitation of the spectrometer time constant of 1 ms in the present study cannot account for the decrease in the signal amplitude caused by Mn^{2+}. The present finding indicates that Y_Z^+ is rapidly reduced by an electron donation from Mn^{2+} that is bound to a unique binding site. In the reported studies, time-resolved measurements proceeded in a redox buffer containing equimolar ferricyanide and ferrocyanide to keep the effective concentration of reactants during repetitive flashes. The assumed rate-limiting step under these conditions might be binding of Mn^{2+} to the site or a redox-buffer-dependent reduction of Mn^{3+} that has to be released from its binding site before rereduction to Mn^{2+}. The diffusion of Mn^{2+} then limits the whole reaction process, and Mn^{2+} will affect the reduction kinetics of Y_Z^+ but not its amplitude. In this context, Y_Z^+ is reportedly reduced biphasically by Mn^{2+} at pH 7.5 (*17*). The fast phase has a lifetime of about 0.3−0.5 ms and it does not depend on Mn^{2+} concentration, but the slow phase accelerates as the Mn^{2+} concentration increases. This may be compatible with the present result, although the dependence of the intensity of these two phases on Mn^{2+} concentration had not been reported.

Several lines of evidence implicate a histidine residue in the binding of Mn^{2+}. Treatment of the Mn-depleted membranes with the histidine modifier diethyl pyrocarbonate (DEPC) partially suppresses the Mn^{2+}-dependent inhibition of DPC-supported DCIP photoreduction (*23, 24*) and changes the pH dependence of the apparent K_M value for Mn^{2+} determined by the rate of DCIP photoreduction with Mn^{2+} as an electron donor (*20*). These results have been interpreted to mean that a histidine residue participates in Mn^{2+} binding in some of the high-affinity sites or some ligands of a single site for Mn^{2+}. As shown in Figure 5B, the pH dependence curve of the dissociation constants of Mn^{2+} is compatible with the view that a histidine residue is involved in Mn^{2+} binding at this unique site. A histidine residue has been proposed to serve a proximal base that receives the phenolic proton of Y_Z (*42*) and/or serve as a ligand for the manganese cluster (*43*). Such a histidine residue may also responsible for the binding of Mn^{2+} by taking into account a rapid (<1 ms) and efficient electron donation to Y_Z^+ from the bound Mn^{2+}.

The pH dependence curve described in this study is quite different from that reported for the apparent K_M value derived from Mn^{2+}-dependent DCIP photoreduction (*20*), in which the pH dependence is represented as a straight line with a slope of −1 between pH 8.0 and 6.2, below which the value becomes less dependent on pH. At present, there is no clear explanation that accounts for this difference in the dependence curves. Modification of the membranes with DEPC in the presence of native manganese cluster does not affect the pH dependence of the K_M value, although a rapid Y_Z^+ reduction by Mn^{2+} was largely inhibited (*20*). Therefore, the K_M may not directly reflect the affinity of the site for Mn^{2+} responsible for Y_Z^+ reduction.

REFERENCES

1. Debus, R. J. (1992) *Biochim. Biophys. Acta 1102*, 269−352.
2. Yachandra, V. K., Sauer, K., and Klein, M. P. (1996) *Chem. Rev. 96*, 2927−2950.
3. Britt, R. D. (1996) in *Oxygenic Photosynthesis: The Light Reactions* (Ort, D. R., and Yocum, C. F., Eds.) pp 137−164, Kluwer Academic Publisher, Dordrecht.
4. Renger, G. (1997) *Physiologia Plantarum 100*, 828−841.
5. Cheniae, G. M., and Martin I. F. (1973) *Photochem. Photobiol. 17*, 441−459.
6. Ono, T.-A., and Inoue, Y. (1987) *Plant Cell Physiol. 28*, 1293−1299.
7. Tamura, N., and Cheniae, G. M. (1987) *Biochim. Biophys. Acta 890*, 179−194.
8. Miller, A.-F., and Brudvig, G. (1989) *Biochemistry 28*, 8181−8190.
9. Zaltsman, L., Ananyev, G. M., Bruntrager, E., and Dismukes, G. C. (1997) *Biochemistry 36*, 8914−8922.
10. Yamashita, T., and Tomita, G. (1974) *Plant Cell Physiol. 15*, 69−82.
11. Ono, T.-A., and Inoue, Y. (1983) *Biochim. Biophys. Acta 723*, 191−201.
12. Tamura, N., Inoue, Y., and Cheniae, G. M. (1989) *Biochim. Biophys. Acta 976*, 173−181.
13. Izawa, S. (1970) *Biochim. Biophys. Acta 547*, 328−331.
14. Velthuys, B. R. (1983) in *The Oxygen Evolving System of Photosynthesis* (Inoue, Y., Crofts, A. R., Govindjii, Murata, N., Renger, G., and Satoh, J., Eds.) pp 83−90, Academic Press, New York.
15. Boussac, A., Picaud, M., and Etienne, A.-L. (1986) *Photobiochem. Photobiophys. 10*, 201−211.
16. Inoue, H., and Wada, T. (1987) *Plant Cell Physiol. 28*, 767−773.
17. Hoganson, C. W., Ghanotakis, D. F., Babcock, G. T., and Yocum, C. F. (1989) *Photosynth. Res. 22*, 285−293.
18. Blubaugh, D. J., and Cheniae, G. M. (1990) *Biochemistry 29*, 5109−5118.
19. Hoganson, C. W., Casey, P. A., and Hansson, Ö. (1991) *Biochim. Biophys. Acta 1057*, 399−406.

20. Magnuson, A., and Andréasson, L.-E. (1997) *Biochemistry 36*, 3254−3261.
21. Nixon, P. J., and Diner, B. A. (1992) *Biochemistry 31*, 942−948.
22. Kullander, C., Fredriksson, P.-O., Sayre, R. T., Minagawa, J., Crofts, A. R., and Styring, S. (1995) in *Photosynthesis: from Light to Biosphere* (Mathis, P., Ed.) Vol. 2, pp 321−323, Kluwer Academic Publishers, Dordrecht, The Netherlands.
23. Preston, C., and Seibert, M. (1991) *Biochemistry 30*, 9615−9624.
24. Preston, C., and Seibert, M. (1991) *Biochemistry 30*, 9625−9633.
25. Hsu, B.-D., Lee, J.-Y., and Pan, R.-L. (1987) *Biochim. Biophys. Acta 890*, 89−96.
26. Klimov, V. V., Allakhverdiev, S. I., Shuvalov, V. A., and Krasnovsky, A. A. (1982) *FEBS Lett. 148*, 307−312.
27. Ghirardi, M. L., Lutton, T. W., and Seibert, M. (1996) *Biochemistry 35*, 1820−1828.
28. Ghirardi, M. L., Preston, C., and Seibert, M. (1998) *Biochemistry 37*, 13567−13574.
29. Ghirardi, M. L., Lutton, T. W., and Seibert, M. (1998) *Biochemistry 37*, 13559−13566.
30. Ananyev, G. M., and Dismukes, G. C. (1997*) Biochemistry 36*, 11342−11350.
31. Tamura, N., Noda, K., Wakamatsu, K., Kamachi, H., Inoue, H., and Wada, K. (1997) *Plant Cell Physiol. 38*, 578−585.
32. Ono, T., and Inoue, Y. (1986) *Biochim. Biophys. Acta 850*, 380−389.
33. Ono, T., and Inoue, Y. (1983) *FEBS Lett. 164*, 255−260.
34. Booth, P. J., Rutherford, A. W., and Boussac, A. (1996) *Biochim. Biophys. Acta 1277*, 127−134.
35. Chen, G., Kazimir, J., and Cheniae, G. M. (1995) *Biochemistry 34*, 13511−13526.
36. Miyao, M., and Inoue, Y. (1991) *Biochim. Biophys. Acta 1056*, 47−56.
37. Ono, T., and Inoue, Y. (1991) *Biochemistry 30*, 6183−6188.
38. Joliot, A., and Joliot, P. (1964) *C. R. Acad. Sci. Paris 258*, 4622−4625.
39. Melis, A., and Homann, P. H. (1978) *Arch. Biochem. Biophys. 190*, 523−530.
40. Yerkes, C. T., Babcock, G. T., and Crofts, A. R. (1983) *FEBS Lett. 158*, 359−363.
41. Shigemori, K., Mino, H., and Kawamori, A. (1997) *Plant Cell Physiol. 38*, 1007−1011.
42. Gilchrist, M. L., Ball, J. A., Randall, D. W., and Britt, R. D. (1995) *Proc. Natl. Acad. Sci. U.S.A. 92*, 9545−9549.
43. Tang, X.-S., Diner, B. A., Larsen, B. S., Gilchrist, M. L., Lorigan, G. A., and Britt, R. D. (1994) *Proc. Natl. Acad. Sci. U.S.A. 91*, 704−708.

BI982949S